Quasi-Static Analysis of Rocking Wall Systems

Douglas Seymour and Simon Laflamme

Department of Civil and Environmental Engineering,
Massachusetts Institute of Technology, Cambridge MA
ds1@mit.edu, laflamme@mit.edu

Abstract: Rocking wall systems consist of shear walls that are free to rotate at their base. Their purpose is to mitigate seismic structural damage by constraining the structure primarily to its first mode. This constraint prevents weak story failure, and maximizes energy dissipation by activating plastic hinges throughout the structure. The purpose of this paper is to present a methodology for the design of rocking wall systems. A quasi-static analysis model is used for predicting the seismic mitigation performance of rocking walls. The stiffness matrix is generalized for an N-story simplified structure equipped with this structural system. The model presented enables optimization of the design parameters, and consequently improved system effectiveness, analytical tractability, and material usage. The method is validated using the case study of an existing rocking wall system installed in a structure located in Tokyo, Japan.

Keywords: Earthquake resistant structures, Earthquake engineering, Seismic analysis, Seismic design

1 Introduction

Maintaining structural serviceability after a seismic event is an increasingly desirable requirement for structural control (Kishiki and Wada 2009). A number of design philosophies have been introduced, such as the performance-based approach (Connor 2003), and damage avoidance design (Mander and Cheng 1997), which share the goal of enforcing effective performance upon a structure subjected to motion. Passive structural control systems have gained popularity for efficiently mitigating energy inputs, which improves the probability of maintaining serviceability in addition to ensuring structural integrity (Laflamme *et al*. 2011). Popular passive dissipation systems include tuned-mass dampers, viscous dampers, base-isolation systems, and hysteretic dampers (Symans *et al*. 2008).

Recently, rocking walls have been proposed (Ajrab *et al*. 2004) and applied (Wada *et al*. 2009) as a passive energy dissipation system. A rocking wall system consists of one or more shear walls that are free to rotate at the base, and that are laterally pin-connected to the structure. Their purpose is to mitigate seismic structural damage by constraining a structure primarily to its first mode. This constraint prevents weak story failure, and maximizes energy dissipation by activating a greater number of plastic hinges. Rocking walls also provide a convenient location to add damping to a structure. The increased energy dissipation that a rocking wall facilitates may be illustrated by comparing local failure modes with the global failure mode, as shown in Fig. 1.

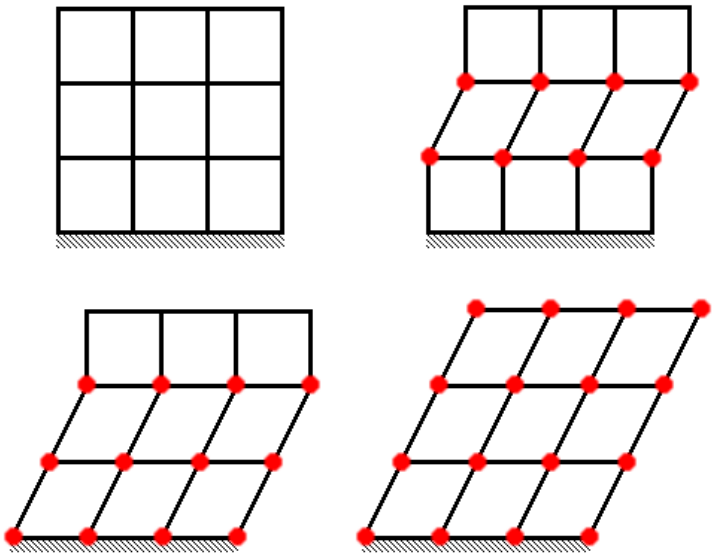

Figure 1. Schematic of a structural frame and its pushover failure modes. Red dots indicate plastic hinges.

It will be readily appreciated that as the number of activated plastic hinges increases, so does the ability of a structure to dissipate energy. The first two failure modes shown in Fig. 1 b) and c) have lower energy dissipation, resulting in larger story drifts with high potential for structural damage or failure. The global failure mode shown in Fig. 1 d) activates all possible plastic hinges, offering the maximum energy dissipation per unit displacement, thus preventing the damaging weak failure modes (Wada *et al*. 2009).

The concept of rocking shear walls was introduced by Ajrab *et al*. (2004). The work presented in that paper built on studies originated by Housner (1963) that investigated the free vibration of rocking blocks. Much work on rocking walls has focused on restoring the moment resistance that is lost at the base of the wall. Many original methods have been proposed. For example, Pekcan *et al* (2000) suggested that anchored tendons be draped through the rocking wall to match the moment distribution induced under the assumed inertial loading. However, current applications of rocking walls have been for retrofit, and thus the critical consideration is the seismic load-bearing capacity of a building, rather than the general lateral load-bearing capacity (Kishiki and Wada 2009).

Following the approach of Housner (1963), early rocking wall models were flat-based. However, flat-based rocking walls may suffer from crushing of the base corners and shock damage, impairing the ability to analytically determine further seismic performance. Wada *et al*. (2009) proposed and implemented an open pin fabricated from cast iron at the base of the rocking wall to prevent this damage, as illustrated in Fig. 2. The addition of the pin removes ground interaction radiation, which was suggested by Ajrab *et al*. as a significant source of damping. However, the high displacement of the rocking wall allows the possibility of controlled damping at the links attaching the rocking wall to the main structure.

Figure 2. Cast iron base hinge to prevent shock damage

The implementation of rocking wall systems is in its infancy. Their design currently requires extensive analysis and experimentation to determine an effective and economical wall size. Tools are required that would reduce the time and effort required for the analysis phase. The benefits of developing analytical and numerical tools for rocking wall systems include enhanced effectiveness of the structural system and its connections to the structure, better understanding of the structural system by an improved analytical tractability, and savings on materials via the optimization of the wall size.

This paper develops tools to assist designers in determining the optimum size of rocking wall for their installation, and to determine the forces in the rocking wall links for their design. This is achieved by the development of a method to determine the relationship between rocking wall size and maximum story drift for an arbitrary building configuration, and to determine the forces in the lateral building-wall links under a given seismic loading. The objective is to improve understanding of these structural systems, and ease their analysis.

Section 2 presents the analytical model for quasi-static analysis of rocking wall systems. Section 3 details its application, introduces illustrative software developed for applying the model, and analyses the results. The section also includes a comparison with a case study of a building retrofitted with rocking walls to the predictions offered by this model. Section 4 discusses the implications of the analysis. Section 5 concludes the paper.

2 Analytical Model

An analytical model of the rocking wall-building system, culminating in the definition of the stiffness matrix, is first derived in this section.

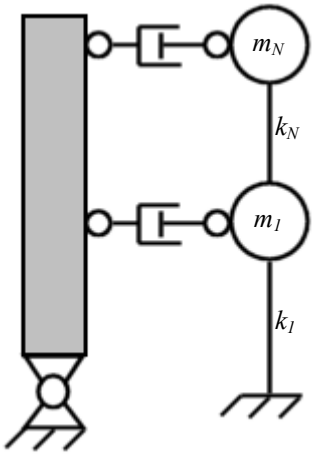

Figure 3. The statically condensed rocking wall-building system to be modeled.

The rocking wall-structure system is illustrated in Fig. 3, in which k_i and m_i represent the stiffness and tributary mass respectively of the i^{th} story. The development of the model begins by representing the rocking wall as a hinged beam, as shown in Fig. 4, in which F_i represent any loading on the beam that is constrained to static equilibrium.

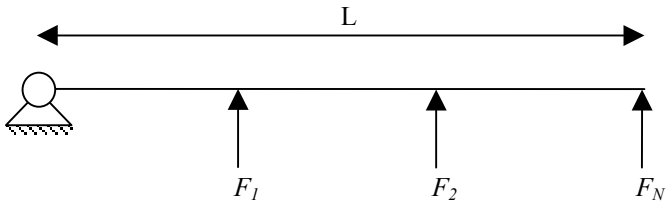

Figure 4. Model of the free rocking wall.

Computing moments about the pin, assuming constant inter-story height for simplicity, and setting the lowermost force to be a function of the others, an expression to describe the link forces F_i is obtained,

$$F_1 = -2F_2 - 3F_3 \ldots - NF_N \qquad (1)$$

These forces may be applied to the beam model in balanced pairs. First F_N at node N with a reaction of $-NF_N$ at position *1*, illustrated in Fig. 5, followed by F_{N-1} at node *N-1* with a reaction of $-(N-1)F_{N-1}$ at position *1*, and so on.

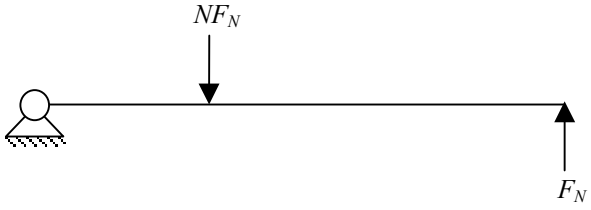

Figure 5. loads applied to the mechanism in pairs, maintaining static equilibrium

It can be shown readily that the order *N–1* wall *pseudo*-flexibility matrix $\boldsymbol{F}_{wall}$ consists of elements:

$$\{\boldsymbol{F}_{wall}\}_{ij} = \frac{aL}{3NEI}x + \frac{x^2}{6EI}(-x + 3a) \quad (i \le j;\ 1 \le i,j \le N\text{-}1;\ \text{i.e. } x \le a) \qquad (2)$$

$$\{\boldsymbol{F}_{wall}\}_{ij} = \frac{aL}{3NEI}x + \frac{a^2}{6EI}(3x - a) \quad (i > j;\ 1 \le i,j \le N\text{-}1;\ \text{i.e. } x > a) \qquad (3)$$

which consist of a rotational term and a cantilever term, and where x and a are *distance to point of measurement* and *distance to point of application of load* from the pin respectively, and obtained as:

$$x = \frac{i\text{-}2}{N}L \qquad (4)$$

$$a = \frac{j\text{-}2}{N}L \qquad (5)$$

Rather than providing the displacements, $\boldsymbol{F}_{wall}$ provides the shape, $\boldsymbol{W} = \boldsymbol{F}_{wall}\boldsymbol{F}_w$, of the wall under the statically-balanced loading $\boldsymbol{F}_w$, where the zero reference line is projected from the pin, through the lowest load-position on the beam, as illustrated in Fig. 6.

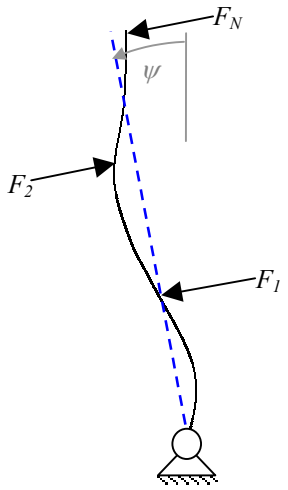

Figure 6. The model beam loaded and deformed. The reference line, shown dashed, coincides with the lowest beam reference position. ψ is the small angle through which the reference line is displaced.

A vector of displacements relative to the reference line may be defined as $\boldsymbol{W}$. The total displacement of the wall is given by $\boldsymbol{W}$, plus a rigid body rotation. For now, let $\boldsymbol{W}$ be of size $N\text{-}1$, omitting the lowest relative displacement $W_1 = 0$. The analysis may be continued by recognizing that since the beam is a mechanism, it may be rotated to any arbitrary small angle ψ under an arbitrary loading, such that the absolute positions of the beam are a rigid body rotation $\boldsymbol{\psi}$, plus the deviations from that line, $\boldsymbol{W}$. Additional information is required to fix the beam in space. Consider the model in figure 7, where $\boldsymbol{U}$, $\boldsymbol{V}$, $\boldsymbol{P}$, $\boldsymbol{Q}$, and $\boldsymbol{F}$ are vectors of displacements of the building and wall, loading on the building and wall, and link forces respectively.

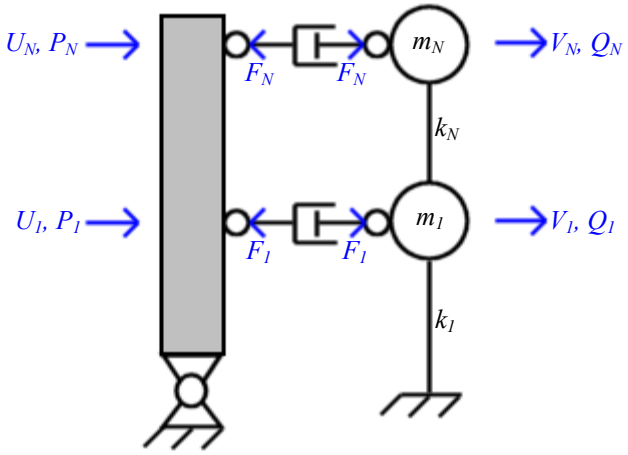

Figure 7. The rocking wall-building system model with forces and displacements required to complete the analysis

From the previous discussion, a matrix $\boldsymbol{F}_{wall}$ that uniquely maps the upper N-1 net forces to the relative displacements of the wall $\boldsymbol{W}$ is determined. Since this mapping is clearly unique, $\boldsymbol{F}_{wall}$ may be inverted to $\boldsymbol{K}_{wall}$. The order of $\boldsymbol{K}_{wall}$ may then be incremented to N, by temporarily adding a leftmost zero column and topmost zero row. Thus $\boldsymbol{K}_{wall}$ now uniquely maps all N relative displacements $\boldsymbol{W}$, including the lowest relative displacement W_1 which is always zero, to the *upper* N-1 forces $\boldsymbol{F}_w$**'** on the wall:

$$\boldsymbol{F}_w' = \boldsymbol{K}_{wall}\boldsymbol{W} \tag{6}$$

The vector $\boldsymbol{F}_w$**'** is denoted prime since it is incomplete: it incorrectly records the force in the lowest position as zero. That force may be determined by applying moments at the pin. A matrix $\boldsymbol{M}_o$ may be formulated which enforces the principle of moments, such that:

$$F_{w,N} = \begin{bmatrix} 0 \\ \vdots \\ 0 \\ F_{w,N} \end{bmatrix} = \boldsymbol{M}_o\boldsymbol{F}_w' \tag{7}$$

where:

$$\boldsymbol{M}_o = \begin{bmatrix} 0 & \dots & -(N-1) & -N \\ \vdots & & & 0 \\ \vdots & & & \vdots \\ 0 & \dots & \dots & 0 \end{bmatrix} \tag{8}$$

Thus the complete net force on the wall is:

$$\boldsymbol{F}_w = \boldsymbol{F}_w' + \boldsymbol{M}_o\boldsymbol{F}_w' = (\boldsymbol{M}_o + \boldsymbol{I})\boldsymbol{F}_w' = (\boldsymbol{M}_o + \boldsymbol{I})\boldsymbol{K}_{wall}\boldsymbol{W} \tag{9}$$

Since the total forces on the wall and on the building are defined as:

$$\boldsymbol{F}_w = \boldsymbol{Q} - \boldsymbol{F} \tag{10}$$

$$\boldsymbol{F}_b = \boldsymbol{P} + \boldsymbol{F} \tag{11}$$

These may be rearranged to:

$$\boldsymbol{F} = \boldsymbol{Q} - \boldsymbol{F_w} = \boldsymbol{Q} - (\boldsymbol{M_o} + \boldsymbol{I})\boldsymbol{K_{wall}}\boldsymbol{W} \tag{12}$$

$$\boldsymbol{F} = \boldsymbol{F_b} - \boldsymbol{P} = \boldsymbol{K_{bldg}}\boldsymbol{U} - \boldsymbol{P} \tag{13}$$

Applying Newton's third axiom, the above two formulae may be equated and rearranged to

$$\boldsymbol{K_{bldg}}\boldsymbol{U} + (\boldsymbol{M_o} + \boldsymbol{I})\boldsymbol{K_{wall}}\boldsymbol{W} = \boldsymbol{P} + \boldsymbol{Q} \tag{14}$$

As discussed, the absolute displacement of the wall is given as:

$$\boldsymbol{V} = \boldsymbol{\psi} + \boldsymbol{W} \tag{15}$$

where $\boldsymbol{\psi}$ is an arbitrary rigid body rotation vector, and $\boldsymbol{W}$ is the relative displacement of each point about that rigid body rotation. If ψ is the scalar angle of rotation, then:

$$\boldsymbol{\psi} = \psi \begin{bmatrix} h \\ 2h \\ \vdots \\ Nh \end{bmatrix} \tag{16}$$

and since the lowest position lies on the line by definition:

$$\psi = \frac{V_1}{h} \tag{17}$$

thus equation (15) becomes:

$$\boldsymbol{\psi} = V_1 \begin{bmatrix} 1 \\ 2 \\ \vdots \\ N \end{bmatrix} \tag{18}$$

or

$$\boldsymbol{\psi} = \boldsymbol{L_1}\boldsymbol{V} \tag{19}$$

where $\boldsymbol{L_1}$ is a linear matrix that acts on the 1st term of a vector:

$$\boldsymbol{L_1} = \begin{bmatrix} 1 & 0 & \dots & 0 \\ 2 & & & \vdots \\ \vdots & & & \vdots \\ N & 0 & \dots & 0 \end{bmatrix} \tag{20}$$

substituting equation (19) into equation (15), it is found that:

$$\boldsymbol{W} = \boldsymbol{V} - \boldsymbol{L_1}\boldsymbol{V} = (\boldsymbol{I} - \boldsymbol{L_1})\boldsymbol{V} \tag{21}$$

which may be substituted into equation (14) to yield:

$$\boldsymbol{K_{bldg}}\boldsymbol{U} + (\boldsymbol{M_o} + \boldsymbol{I})\boldsymbol{K_{wall}}(\boldsymbol{I} - \boldsymbol{L_1})\boldsymbol{V} = \boldsymbol{P} + \boldsymbol{Q} \tag{22}$$

If damping is to be added between the wall and the building, $\boldsymbol{U}$ and $\boldsymbol{V}$ must be considered independent. However, damping is outside of the scope of this paper, as we are considering quasi-static loading. Without damping, it may be assumed that the links are rigid, and thus that the building displacements $\boldsymbol{U}$ are equal to the wall displacements $\boldsymbol{V}$. Thus the stiffness matrix of the undamped system is given as:

$$[\boldsymbol{K}_{bldg} + (\boldsymbol{M}_o + \boldsymbol{I})\boldsymbol{K}_{wall}(\boldsymbol{I} - \boldsymbol{L}_1)]\boldsymbol{U} = \boldsymbol{P} + \boldsymbol{Q} \quad (23)$$

where $\boldsymbol{P} + \boldsymbol{Q}$ are the combined loads on the system, and the matrices are as previously defined.

Using the displacements found with equation (23), equation (11) may be rearranged to find $\boldsymbol{F}$, the forces in the links:

$$\boldsymbol{F} = \boldsymbol{F}_b - \boldsymbol{P} = \boldsymbol{K}_{bldg}\boldsymbol{U} - \boldsymbol{P} \quad (23)$$

This measure of the link forces should generally be considered as an upper bound, since applying the loads in a quasi-static fashion implicitly discounts any additional damping that may be added to a rocking wall installation.

3 Analysis

The analytical stiffness matrix derived in the previous section can be used to determine functions of story drifts with respect to wall width for any arbitrary building configuration. The most widely understood method of applying seismic loads is the ASCE 7 (2005)/IBC building code static equivalent method.

A function of maximum story drift with respect to wall width, for an arbitrary building configuration, can be obtained by discretizing the wall at each floor using tributary areas, iteratively changing the wall size and corresponding seismic load, and finding the set of story drifts.

The authors have developed illustrative software which accomplishes the above, accepting as input the basic information about a structure that a designer would input into any seismic load calculating software, and providing as output MATLAB- and spreadsheet-ready data that gives the designer relevant information about rocking wall requirements, including the design function of maximum story drift with respect to wall width.Tests of the analytical building-rocking wall model, presented in section 1, against linear finite element models have shown that the two match exactly.

A number of simplified benchmark buildings up to 15 stories tall were designed to analyze their interaction with a variety of rocking wall systems, under quasi-static seismic loading. For these benchmark buildings, a stiffness distribution factor *d=25%* represents a linear stiffness distribution where each story stiffness increases by 25% of the top story stiffness. A large number of functions of maximum story drift against rocking wall width were plotted for the benchmark buildings, and a case study building to be discussed later. Illustrative examples of the functions found may be seen in Fig. 8.

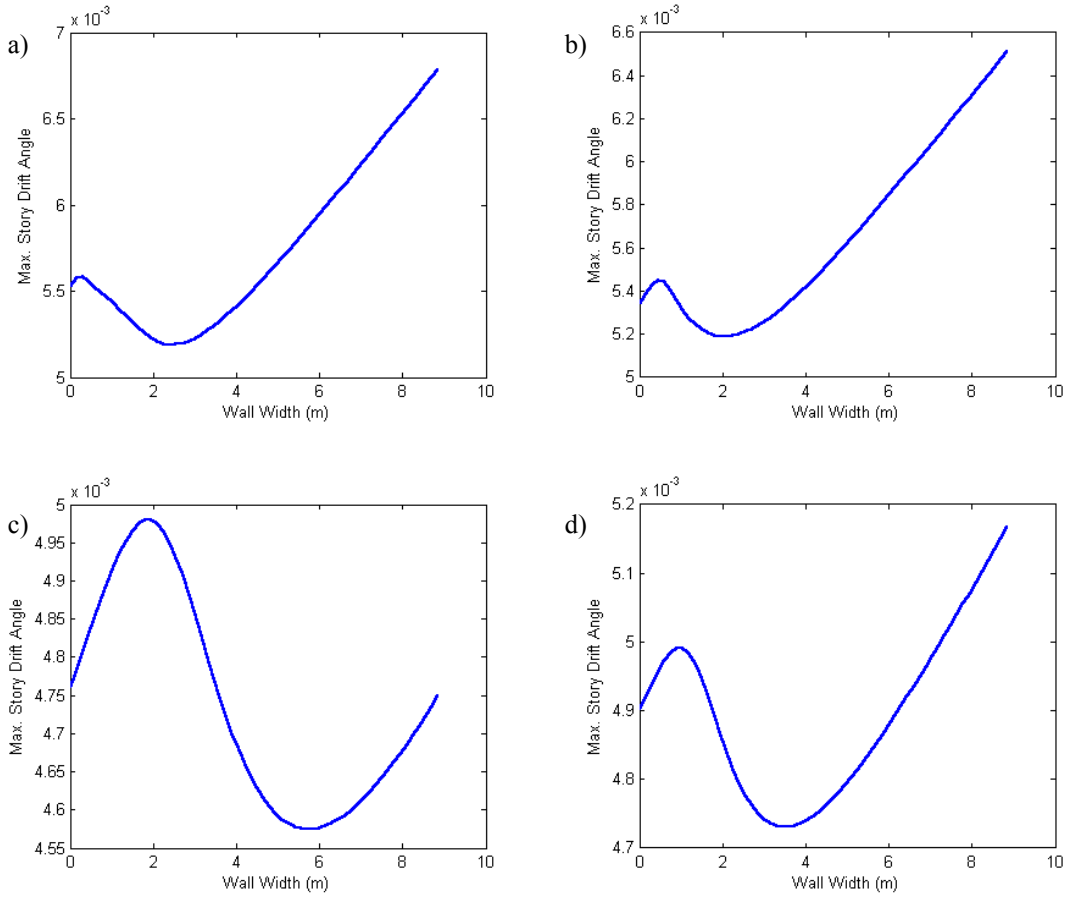

Figure 8. Functions of inter-story drift angle vs. wall width, where two identical rocking walls are used. The benchmark buildings represented have the characteristics a) *N=6, d=100%*; b) *N=7, d=50%*; c) *N=9, d=0%*; d) *N=10, d=25%*

It is clear from these functions that the presence of counteracting effects in rocking wall installations, most notably the counteracting effects of increasing mass and stiffness, consistently provide minima and maxima in these functions. As hypothesized, there may be many opportunities to design optimum rocking walls that take advantage of these functional minima. It is also noted that points of diminishing returns occur before the minima in these functions, enabling a designer to choose an economically optimal wall size.

3.1 Case Study: Tokyo Institute of Technology, Building G3

In order to test the hypothesis that these function minima represent useful data points at which to design rocking walls, a case study is considered. The case study chosen is the G3 building at the Tokyo Institute of Technology, which was retrofitted with six rocking walls, as discussed in detail in Wada *et al*. (2009). Figs. 9-11 describe the building. Fig 9 shows a sketch of the building, Fig. 10 illustrates the plan view, and Fig. 11 is a photograph of a central wall, as installed.

Figure 9. A model of the retrofitted case study building. Yellow represents new structure. (Wada *et al*. 2009)

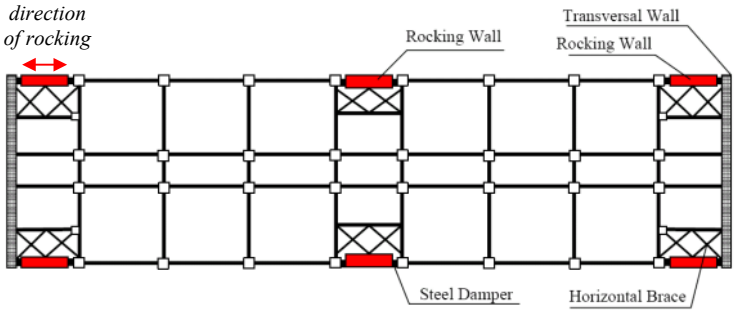

Figure 10. A plan view of the retrofitted case study building. Red rectangles represent rocking walls. (adapted from Wada *et al*. 2009)

The design proposed by Wada *et al*. consists of wide and shallow rocking walls (14.4ft by 2ft in plan) that rock in the longitudinal direction of the building. The rocking walls add 56% to the existing reinforced concrete area in plan. The design of the rocking walls used in the case study was subject to extensive experimentation and data gathering.

The designer may choose the wall thickness to be the minimum thickness required which maintains the wall's inherent stability. In this case, a thickness of 2ft was chosen for an 11-story wall. High stiffness, and thus second moment of area in the direction or rocking, is the core requirement to enforce the desirable fundamental mode response, and thus width is the key design variable.

The wall is prestressed to allow for the large tensile forces which will result from inertial motion, and is designed to remain elastic during severe earthquakes. As illustrated in Fig. 10, this retrofit stiffens the seismic response at six approximately evenly-distributed locations. The existing beam stiffness between the rocking walls ensures that the response between the rocking walls is close to the response at the rocking walls themselves.

Figure 11. A central rocking wall as seen from the ground

The analytical model developed for analyzing the case study building uses an stiffness distribution factor of *d=25%* per story. A plot of the model stiffness with respect to the case stiffness shows an acceptable match, as seen in Fig. 12.

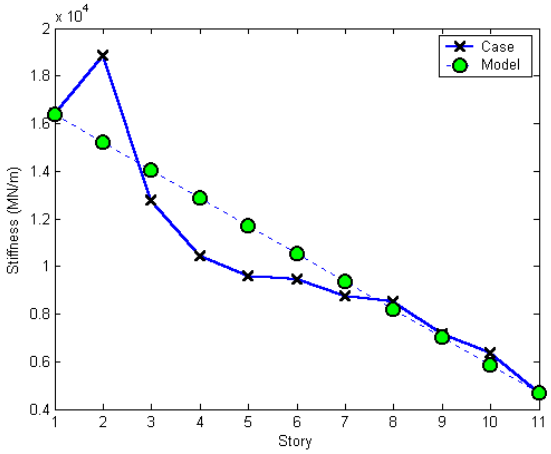

Figure 12. The case building story stiffnesses compared with the linear model

A tributary area mass model is used. The total mass is divided by the number of stories, and distributed equally between the stories. The top floor mass is halved. The model again compares favorably with the case data, as seen in Fig. 13.

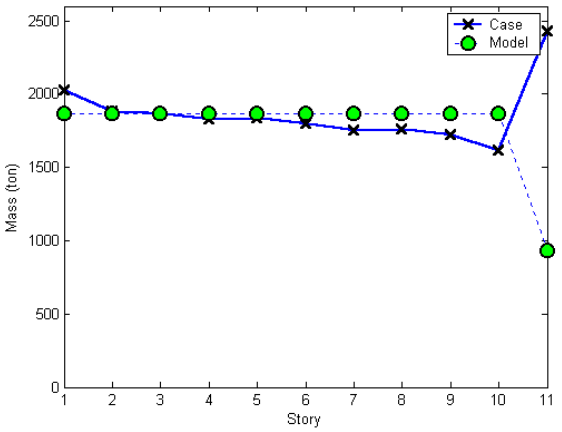

Figure 13. The case building story masses compared with the top-light constant model

The principles developed in this paper may be applied to any arbitrary set of building story stiffnesses and story masses. For simplicity, linearized models have been used thus far.

The natural period of the case study building in the x direction is *0.589s*. The building top stiffness k_N in the x direction is 4.68GN/m. If an inverse-iterated Rayleigh quotient (Chopra 2006) is applied to the linearized mass and stiffness matrices illustrated in Figs. 12 and 13, a first period of *0.539s* is found, which is just *8.7%* less than the theoretical value obtained from engineering data.

This closely-matching model of the case study building, using six rocking walls and a wall depth of *0.61m* as the for the retrofit reported in Wada *et al*. (2009), is used to generate a maximum story drift function with respect to wall width, as described in section 2. The earthquake intensity parameters used in this design are used to generate seismic loads as aforementioned. The model described above produces the function of story drift vs. wall width shown in Fig. 14.

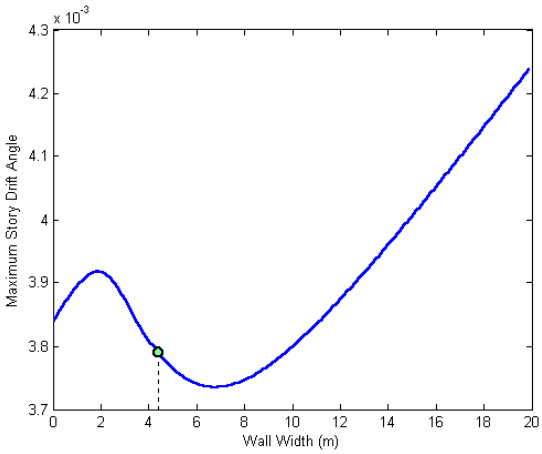

Figure 14. Maximum story drift angle of the modeled case study building, against rocking wall width (m), using 6 rocking walls. The location of the 4.39m-wide walls used in the case study is marked.

Based on the pseudo-static analysis developed in this paper, the choice of six *4.4m*-wide walls was ideal for the Tokyo Institute of Technology G3 building retrofit project. The size chosen maximizes the advantage of a dip in the function relating maximum story drift to wall width, which occurs due to the opposing effects of stiffness and mass. It can be seen from Fig. 14 that although the actual minimum of the function is at *7m*, the returns associated with increasing the wall width begin to diminish significantly after around *4.5m*, as the inertia of the increased mass begins to dominate over the increased stiffness.

By applying the system stiffness matrix derived, under the maximum seismic design loading, it is found that the maximum force in the building-rocking wall links with a wall width of 4.39m as in Fig. 14 is

approximately 28MN for the case study building, and occurs at the second story from the top. This maximum link force is of the order of the weight of one discretized floor.

As previously discussed, this value should be considered to be an upper bound as additional damping is not taken into account. Since the link forces are approximately proportional to lateral displacement, one possible approach to account for damping is to scale the link forces, by the amount by which damping diminishes displacement. Clearly the links, and structure surrounding the wall, require significant strength to withstand such loads. The designer will wish to ensure that the rocking wall engages only strong structural elements.

4 Discussion

The static analysis presented in this paper is straightforward to implement. It is not intended to give a complete picture about the complex dynamic effects occurring in a seismic shaking of a structure. The model offers researchers and designers a clear place to start the analysis process for rocking wall design.

It is worth mentioning that in the case study the maximum story drift occurs at the sixth story from the ground. When the story stiffnesses increase approximately linearly (*d* is approximately 25% in the case study), the maximum story drift due to the seismic equivalent loading often occurs at the middle stories, as seen in Fig. 15. If a parabolic stiffness is applied at the design stage, then the drift profile will be linear without the assistance of a rocking wall (Connor, 2003).

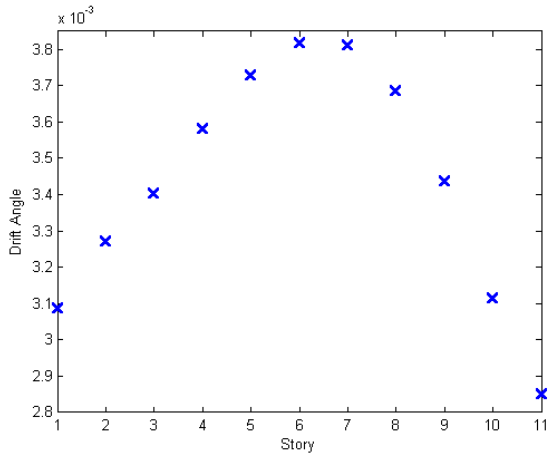

Figure 15. The story drift angles of the case study, with the maximum occurring at the 6th story.

The overall shape of the design graph (Figs. 8, 14) is found to be largely insensitive to small changes in the general dynamic properties of the structure. If the story stiffnesses or masses are changed some reasonable amount, the overall shape of the graph remains very similar, with a non-significant x-axis movement of minima or points of diminishing returns, as shown in Fig. 16.

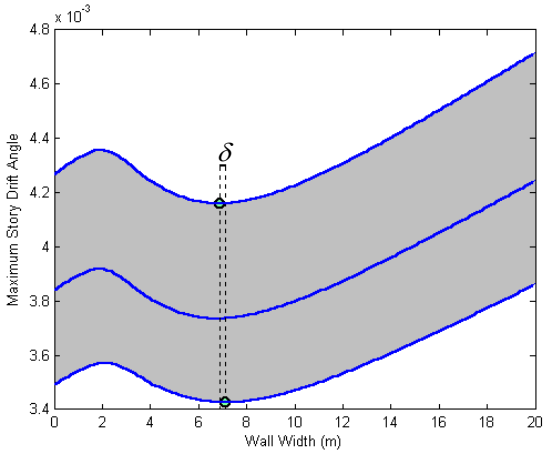

Figure 16. The rocking wall design function of the case study building compared to cases where all story stiffnesses are modified ±10%. The central line is the case study, the upper with stiffnesses decreased by 10%, and the lower with stiffnesses increased by 10%. The change in the minimal width δ is only 0.2m.

Thus, although approximations of a non-exact stiffness and mass profile have been incorporated, there can be confidence that the result returned for most effective size of rocking wall would be very similar even if the fully analytical mass and stiffness matrix of the building had been used. The same is true if the loads are scaled significantly, for example by changing the location and thus the magnitude of the equivalent seismic loads.

5 Conclusion

In this paper, a quasi-static analysis method for rocking wall systems has been developed. The stiffness matrix that is generalized for an *N*-story simplified structure equipped with the passive control system is an accurate simplified model under arbitrary loading.

Based on comparison with the Tokyo Institute of Technology G3 building rocking wall installation, the method presented of using an analytical model to produce a graph of maximum story drift against rocking wall size is an effective way to estimate the size of rocking wall required for a retrofit project.

The software developed for analysis and design of rocking wall systems is a promising tool for enhancing their implementation and creating more efficient structural systems.

Acknowledgement

The authors thank Professor Akira Wada and, Dr. Zhe Qu from the Tokyo Institute of Technology for their valuable support.

References

Ajrab, J., Pekcan, G., and Mander, J. (2004) *Rocking Wall–Frame Structures with Supplemental Tendon Systems.*

American Society of Civil Engineers (2005) *Minimum Design Loads for Buildings and Other Structures, ASCE/SEI 7-05.*

Chopra, A. (2006) *Dynamics of Structures.* Prentice Hall

Connor, J. (2003) *Introduction to Structural Motion Control.* Pearson Education, Upper Saddle River

Kishiki, S. and Wada, A. (2009) *New Dynamic Testing Method on Braced-Frame Subassemblies.*

Housner (1963). *The behavior of inverted pendulum structures during earthquake*. Bull. Seismol. Soc. Am., 53(2), 403–417.

Laflamme, S., Taylor, D., Abdellaoui-Maane, M., and Connor, J. *Modiend friction device for control of large-scale systems*. Structural Control & Health Monitoring (2011).

Mander, J. and Cheng, C-T., (1997). *Seismic resistance of bridge piers based on damage avoidance design*. *Tech. Rep. NCEER-97-0014*, National Center for Earthquake Engineering Research, Buffalo, N.Y.

Pekcan, G., Mander, J., and Chen, S. (2000). *Balancing lateral loads using tendon-based supplemental damping system*. *Journal of Structural Engineering,* 126(8), 896–905.

Symans, M., Charney, F., Whittaker, A., Constantinou, M., Kircher, C., Johnson, M., McNamara, R., et al. *Energy dissipation systems for seismic applications: Current practice and recent developments*. Journal of Structural Engineering 134 (2008), 3.

Wada, A., Qu, Z., Ito, H., Motoyui, S., Sakata, H. and Kasai, K. (2009) *Seismic Retrofit Using Rocking Walls and Steel Dampers.*

The software referenced herein, an example MATLAB code to determine the stiffness matrix derived in section 2, and further information about the benchmark buildings used in the simulations may be accessed at *www.rocking-wall.com*.